A COMPARISON OF FRICTION STIR PROCESSING OF MILL ANNEALED AND INVESTMENT CAST Ti-6Al-4V



A.L. Pilchak [1] **M.C. Juhas [2]** **J.C. Williams [3]**

Department of Materials Science and Engineering, The Ohio State University (United States)

E-mail: [1] pilchak.1@osu.edu, [2] juhas.1@osu.edu, [3] williams.1726@osu.edu

ABSTRACT

Friction stir processing (FSP) of cast and mill annealed Ti-6Al-4V was studied to determine whether this thermo-mechanical processing technique is feasible for local microstructural modification to improve fatigue properties for aerospace engine applications. The ability to produce a friction stir processed surface layer is thought to provide a microstructure that is more resistant to fatigue crack initiation than the as-cast microstructure of the bulk. FSP resulted in a microstructure of either very fine equiaxed α or a colony microstructure with refined prior β grains when processing occurred below the β transus or above the β transus, respectively. The final microstructure observed in the stir zone was related to the processing conditions and was independent of the initial cast or wrought microstructures. Electron backscatter diffraction was used to assess the presence of microtexture in the stir zone. There was very little microtexture observed in sub-transus processed material. A moderate strength α phase texture was observed in the cast and wrought materials processed above the β transus. Fatigue tests performed on 4-point bend samples revealed a dramatic increase in fatigue life after FSP in both mill annealed (presented here) and cast + hot isostatic pressed materials (previously presented) although only a limited number of samples were available. Substantial tool wear is an issue and tungsten contamination is readily observed when FSP temperatures were below the β transus. This could be a concern in high temperature applications or for applications requiring post-processing heat treatment.

IIW-Thesaurus Keywords: *Castings; Cracking; Defects; Fatigue cracks; Fatigue improvement; Microstructure; Reference lists.*

1 INTRODUCTION

Ti-6Al-4V investment castings are widely used in the aerospace industry as replacements for fabrications. These fabrications are made by joining multiple, smaller wrought components together, either mechanically or by welding. The castings have a very coarse microstructure that is not effective against fatigue crack initiation (FCI), yet it is the most fatigue crack growth resistant morphology of $\alpha + \beta$ titanium microstructures. FCI is compromised by the long slip lengths that are associated with the α colonies, which are on the order of several hundred microns in slowly cooled castings. At small crack lengths, where only colony boundaries are strong obstacles to crack growth, large colonies are detrimental to fatigue crack growth rates [1]. At longer crack lengths, however, crack growth resistance increases with increasing colony size. The macrocrack growth resistance arises from roughness induced clos-

Doc. IIW-1888-08 (ex-doc. III-1435r1-07) recommended for publication by Commission III “Resistance welding, solid state welding and allied joining processes”.

ure effects that are observed when the load ratio, R, is small enough to permit crack closure. In this mechanism, plastic deformation or slip irreversibility ahead of the crack tip causes a displacement of fracture surface features on the upper and lower crack faces. When the crack closes these features no longer fit together neatly. Local compressive stresses are developed in the regions where the displaced fracture surface features contact each other during closure. These closure stresses cancel some of the far field applied stress and drive down the effective stress intensity range, ΔK [2].

In the absence of compressive residual stresses, most fatigue cracks initiate at the surface of a component. Therefore, it would be appropriate to transform the surface microstructure into a more crack initiation resistant morphology. Friction stir processing (FSP) has proven to be an effective method of thermomechanically processing specific regions of a component [3, 4]. Since there is no need to weld a joint, the depth of penetration becomes a processing variable. Changing the tool plunge depth can affect the total heat input into the processed material. In titanium alloys, which experience an allotropic phase transformation during heating and cooling, changing the maximum processing temperature can alter the resultant microstructure. The microstructure is an indicator of the maximum processing temperature relative to the β transus [5]. During FSP of Ti-6Al-4V, two different classes of microstructures can be produced. These consist of either fine equiaxed α grains on the order of 1 μm or a colony $\alpha + \beta$ structure within approximately 30 μm prior β grains. In cast Ti-6Al-4V, these two microstructures have been shown to improve the fatigue life over cast microstructures by about an order of magnitude [6, 7]. This behaviour is believed to be due to the reduction in the effective slip length of the material near the surface of the plate. This makes dislocation motion more difficult, reduces the rate of damage accumulation and delays FCI. FSP has been used to heal residual near surface casting porosity in nickel-aluminium-bronze propeller alloys [8-11]. In a similar fashion, we predict that FSP can be used to heal fatigue cracks that are found during inspection of wrought and cast products to extend service life.

2 MATERIALS AND EXPERIMENTAL PROCEDURE

In this study, cast and mill-annealed (wrought) Ti-6Al-4V plates were friction stir (FS) processed using two different tungsten-based tools [5]. The processing conditions are shown in Table 1. It is noted that the cast plate was processed at temperatures below the β transus (sample ID: Cast α/β) and at temperatures that exceeded the β transus (sample ID: Cast β), while the mill-annealed plate was only β – FS processed. Argon shielding gas was used to limit oxygen contamination of the work piece. The cast α/β plate was processed in load control and therefore the plunge depth was estimated from optical and scanning electron microscope (SEM) images. The cast and β – FS processed and the mill-annealed and β – FS processed plates were processed in depth control so the downforce was an average value during steady state FS processing conditions. The exact thermomechanical history of the mill-annealed plate is unknown, but a metallographic section transverse to the rolling direction has a bi-modal microstructure containing ~ 25 μm equiaxed α grains with similarly sized, or slightly smaller, colony $\alpha + \beta$ [Figure 1 a)]. There is a higher volume fraction of

Table 1 – Friction stir processing parameters used in this study

Sample ID	Travel speed mm s^{-1}	Rotational speed rev min^{-1}	Plunge depth mm	Downforce kN
Cast α/β	0.85	100	~1.8	16.45
Cast β	0.85	150	2.54	~15.20
Mill annealed β	0.85	150	2.54	~14.41

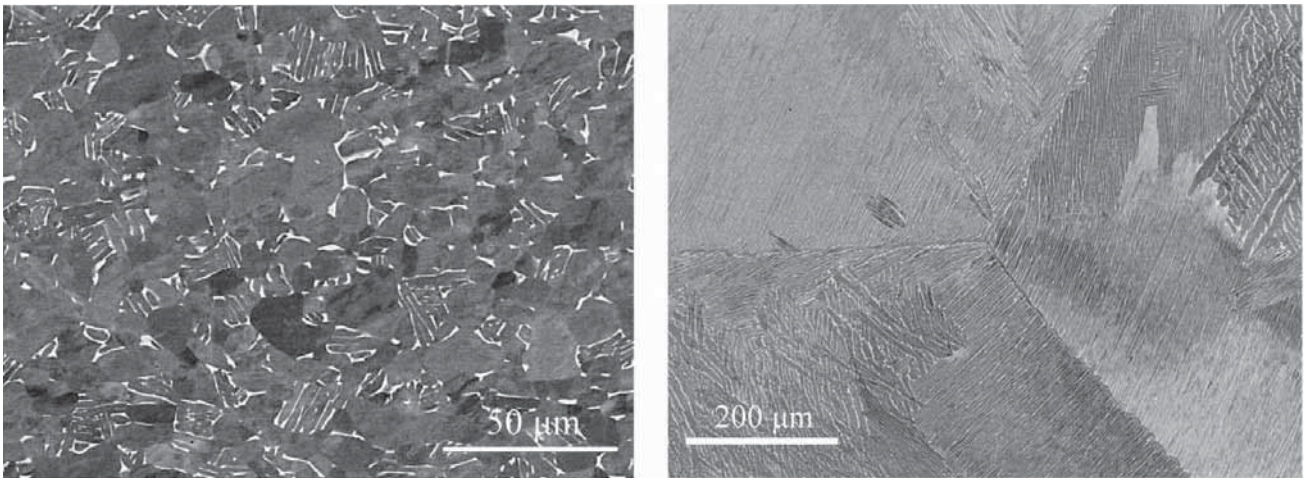

a) As received mill-annealed alloy **b) As-cast + hot isostatically pressed alloy**

Figure 1 – The microstructure in the Ti-6Al-4V alloys used in this study

equiaxed α grains compared to α colonies, so there are many α/α boundaries. This is typical of mill annealed material that is α + β rolled followed by a 700 °C stress relief anneal. The as cast Ti-6Al-4V was hot isostatic pressed (HIP'd) and subsequently annealed at 845 °C for two hours and slowly cooled. The HIP cycle appeared to heal all internal casting porosity. The microstructure consisted of very coarse prior β grains with packets of aligned α lamellae that are separated by thin β ribs. The similarly oriented packets of lamellae share the same crystallographic orientation and collectively with the β phase are known as α colonies. The prior β grain and α colony sizes were on the order of 1.5 mm and 500 μm, respectively [Figure 1 b)].

Electron backscatter diffraction (EBSD) was used to determine local crystallographic orientations using a SEM equipped with a field emission source operated at 20 kV, spot size 5 at a working distance of 21 mm. Four point bend fatigue tests, with the stir zone (SZ) in maximum tension, were performed using a servo-hydraulic frame and reported in previous studies [6, 7]. An additional seven samples were tested and will be reported in the present study. The maximum tensile stress on the surface of the specimens, the load ratio and the frequency were 775 MPa, 0.1 and 20 Hz, respectively.

3 RESULTS AND DISCUSSION

3.1 β – FS processed microstructure

When processed above the β transus, both the bimodal and fully lamellar base material microstructures were transformed to approximately 30 μm prior β grains with α + β colonies that were about half the β grain size (Figure 2). In both cases, continuous recrystallization in the β phase field resulted in a reduction of the β grain size in the SZ. After the tool passed and there was no further deformation, the temperature decreased slowly into the α + β phase field where there was subsequent nucleation and growth of grain boundary α and colony α from the prior β grain boundaries. The prior β grains typically had between two and four α variants present. The cooling rate was limited, except near the surface, by the thermal conductivity of the workpiece, which is quite low for Ti alloys. The surface of the plate was quenched somewhat by the flowing Ar stream. There was no α case formation on any of the samples in this study, which indicated that the Ar gas effectively shielded the surface from oxygen contamination. The grain size near the surface of the plate was more refined compared to those deeper in the SZ, presumably due to the fact that higher strains were imposed near the surface by the shoulder of the tool, which led to an increase in the number of nucleation sites. The observation that the SZ microstructure was the same in both plates that were β – FS processed supports previous work on β-annealed and mill-annealed Ti-6Al-4V that showed the SZ microstructure depended on the processing parameters and not the base material microstructure [5, 12, 13].

Two extremes in the mill-annealed material, the "low" and "high" heat-affected zones are shown in Figure 3. In the low HAZ, the α colonies were the first to dissolve because they were the leanest in β stabilizers due to an element partitioning effect [1]. In the high HAZ, there were no more α colonies present and the size of the

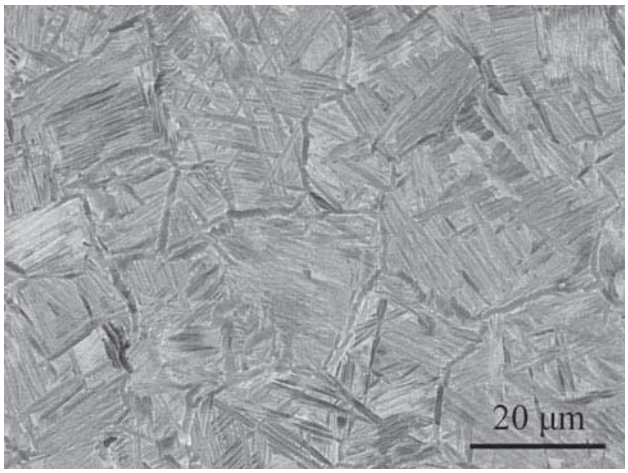

This is also representative of the mill-annealed and β – FSP microstructure.

Figure 2 – The microstructure in the cast and β – FSP condition

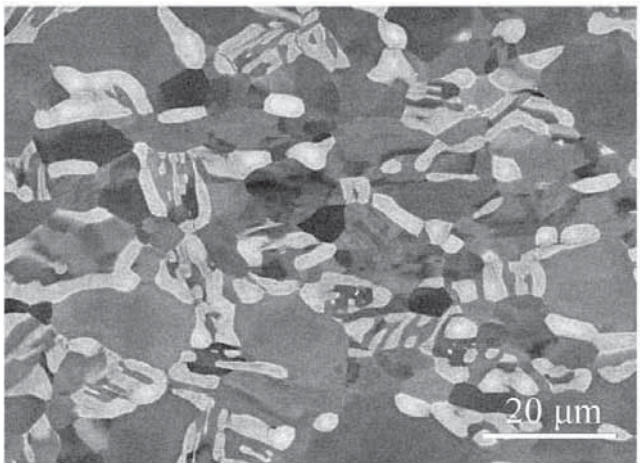

a) Low HAZ

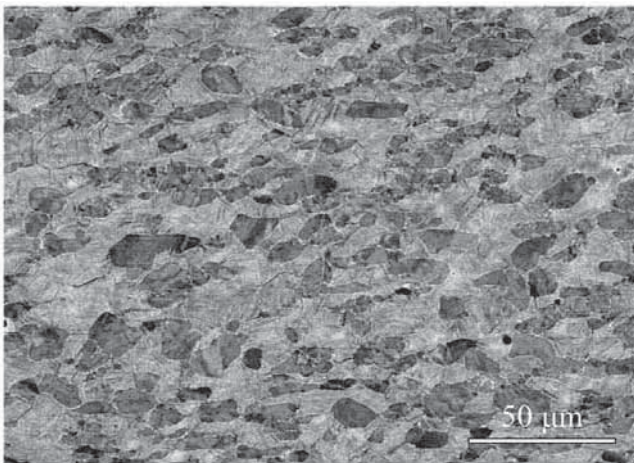

b) High HAZ

Figure 3 – The heat-affected zones in the mill-annealed and β – FSP material

primary α grains had decreased slightly compared to the starting material.

The transition zone (TZ), which is between the SZ and the heat-affected zone (HAZ), was quite different from the SZ microstructure and did depend on the starting material microstructure. The TZ contains both recrystallized grains, as well as remnant starting material microstructure [14]. Mill-annealed products generally have residual stress from processing that can contribute to microstructural evolution in the TZ and HAZ. This made it more difficult to define these regions because there was no clear interface between the TZ and HAZ, but instead a gradual change.

The mill annealed TZ near the SZ consisted of coarse equiaxed α grains, clusters of finer 2 µm – 3 µm equiaxed grains and 10 µm to 20 µm α colonies [Figure 4 a)]. The coarse α grains were slightly smaller than the primary α grain size in the starting material. There was evidence of orientation contrast among the finer α grains (Figure 4b). When the fine α grains were investigated with EBSD, most boundaries had misorientation angles exceeding 15°. The residual strains in the TZ led to lower confidence intervals in the transformed β and retained β regions of the TZ, as shown in the image quality (IQ) map in Figure 5. The darker regions in IQ maps corresponded to the regions of higher residual strain [15]. Most of the equiaxed grains had brighter colours indicating that the plastic deformation was mostly accommodated by the now-transformed β regions. The grain boundary misorientations between a few of the equiaxed grains are also shown. The local misorientations between α grains within the same cluster were quite random, ranging from subgrain boundaries (2°) to high angle grain boundaries. The basal planes in the equiaxed grains with smaller misorientations suggested they were originally from the same primary α grain that was subdivided during FSP. A gradual shift from low angle to high angle boundaries was observed in the TZ with increasing proximity to the SZ in α + β – FS processed material [16]. This is similar to the mechanism of fine grain formation based on continuous dynamic recrystallization in Al alloys that

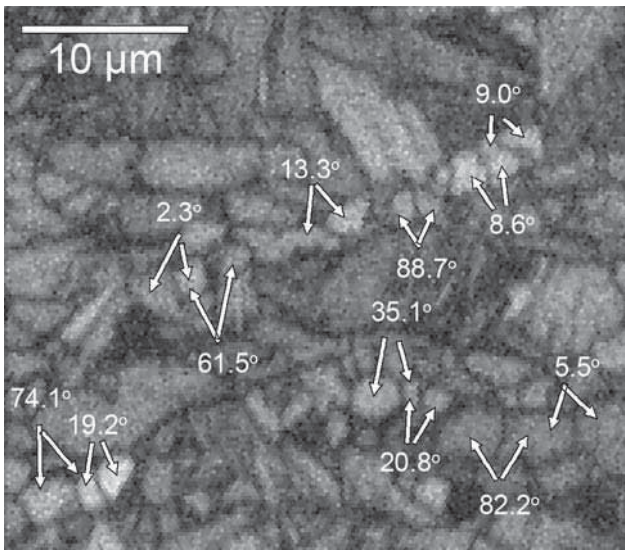

The bright areas correspond to those with low defect density [15]. Local grain boundary misorientations are also shown for several of the equiaxed grains.

Figure 5 – Image quality map of a region in the transition zone of the mill annealed and β - FSP material

was proposed by Su *et al*. [17]. In this model, low angle subgrain boundaries form by dynamic recovery processes ahead of the tool in the TZ and continued deformation causes these subboundaries to rotate to high angle boundaries as dislocation density increases.

The most interesting misorientations were those around 60° and 80° – 90°. Bieler and Semiatin [15] observed similar misorientations of fine grains relative to their parent grain orientation in a Ti-6Al-4V upset forging. The equiaxed α grains were misoriented by 60° or 80-90° from the reference grain orientation. This was related, although not definitively, to a variant selection process being dominant over the epitaxial transformation back to the parent orientation. A potential mechanism was proposed in which there was slip on a (110)β plane that did not initially contain the basal plane before the α → β transformation. This resulted in remnant dislocations on that (110)β plane. Previous studies identified

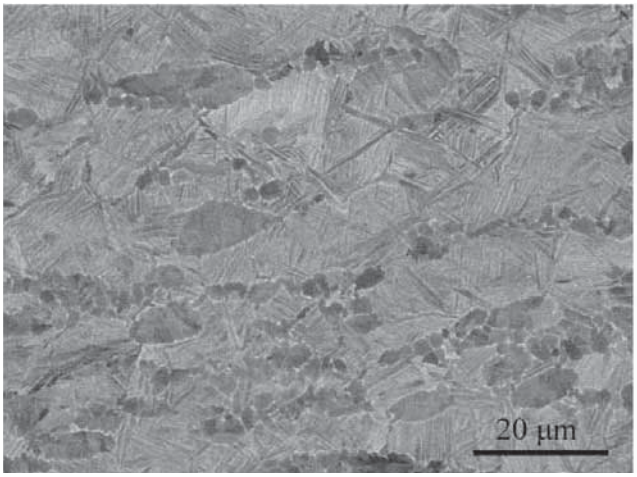

a) The transition zone in the mill-annealed and β – FSP material

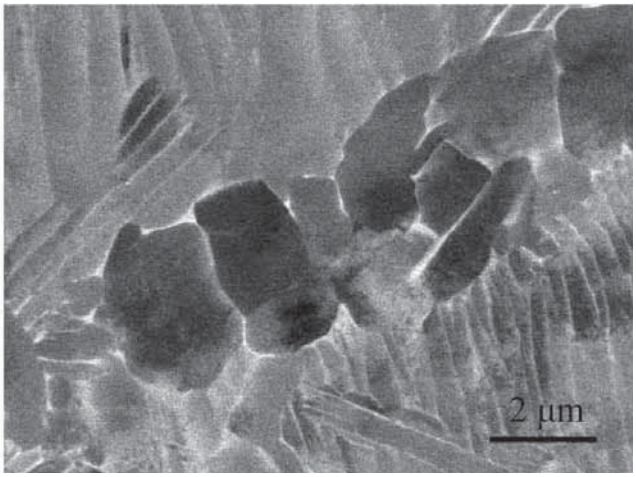

b) A higher magnification showing orientation contrast in the clusters of fine α grains

Figure 4

this as a factor that influences the variant selection process [18, 19]. During the subsequent $\beta \rightarrow \alpha$ transformation, the basal plane in the α phase became parallel to the (110)β plane with the remnant dislocations. The results of this work supports those of Bieler and Semiatin, although it is agreed with those authors that additional work is necessary to fully understand this phase transformation mechanism.

The TZ in the cast α/β – and β – FS processed plates were generally similar and more distinct than in the mill annealed plate, so they will be discussed together. Both contained a combination of deformed α lamellae with equiaxed α grains (Figure 6). The lamellae were curved towards the direction of material flow. There is a higher volume fraction of transformed β in the β – FS processed condition due to the higher peak temperature. The morphology of the transformed β was also different. In the cast and α/β – FS processed material, there were fine-scale α laths, where each individual lamella seems to be one variant. However, in the cast and β – FS processed sample, the transformed β consisted of α colonies where several laths were aligned and shared a common variant. This suggests that the cooling rate in the TZ of the β – FS processed plate was slower. The TZ did not exceed the β transus in either of the β – FS processed plates, as evidenced by the untransformed α in the mill-annealed material and the α lamellae in the cast material. The heat-affected zones in the cast plates were also similar to each other and were characterized by an increased volume fraction of β with a lamellar transformation product between the primary α lamellae.

3.2 α/β – FS Processed Microstructure

In contrast to the β – FS processed cast and wrought material, the SZ in the α/β – FS processed casting (Figure 7) has a primary α grain size on the order of 1 μm. Grain size strongly influences material properties, especially high cycle fatigue strength. Reducing the α grain size from 12 μm ~ 15 μm to 1 μm ~ 2 μm in an equiaxed Ti-6Al-4V alloy corresponded with about a 25 % increase in fatigue strength at 107 cycles [20]. In practice, it is difficult to achieve such uniform fine grains throughout the bulk of a material except for laboratory scale specimens because of the extreme amount of deformation that is required. Thus, FSP offers a cost effective, reproducible manufacturing method of producing a refined, equiaxed microstructure in these materials. Another method, equal channel angular extrusion, is capable of producing 500 nm equiaxed grains Ti-6Al-4V [21]. However, the authors reported that such high strains led to the formation of intense crystallographic textures. A strong texture (10x random) was developed with the basal poles approximately 61° from the extrusion direction corresponding to the maximum shear plane for the test configuration. This can compromise mechanical properties along particular directions due to the inherent elastic and plastic anisotropy of the α phase in titanium alloys. During loading, for example, these regions of preferred orientation could lead to the formation of intense shear bands that are sites for fatigue crack initiation [1].

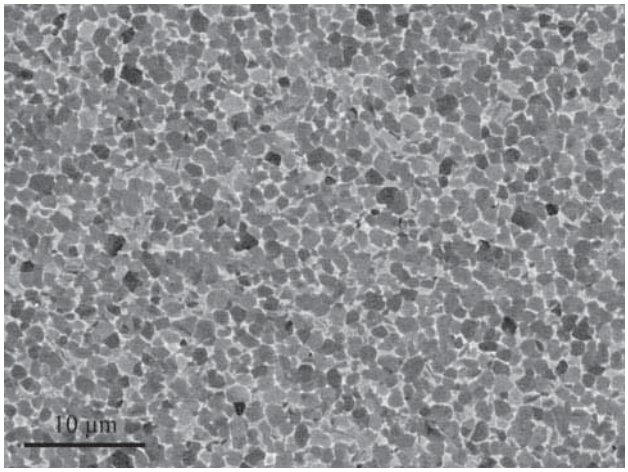

Figure 7 – The microstructure in the stir zone of the cast and α/β – FSP material

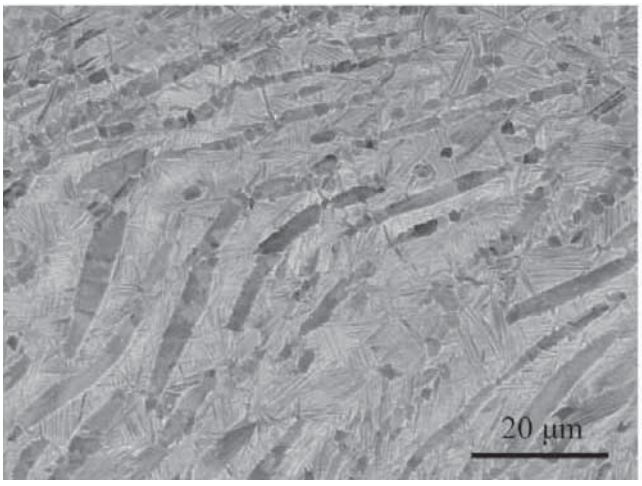

a) in the cast and β – FSP material

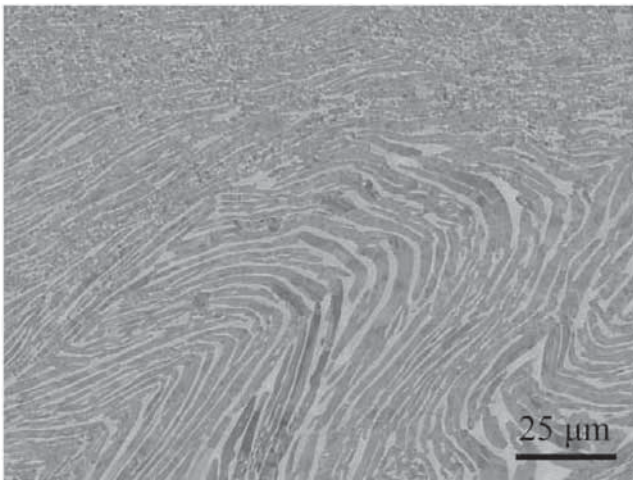

b) in the cast and α/β – FSP material

Both contained a combination of deformed lamellae and equiaxed grains. Note the higher volume fraction of transformed β (lighter coloured phase) in a).

Figure 6 – The transition zone

3.3 Texture analysis

The EBSD scans in this study were performed to assess the degree of microtexture present in these samples. Microtexture can result in the formation of shear bands if there are large regions of similarly oriented grains which can compromise mechanical properties. The EBSD scans were collected from the mid-plane of the SZ on the advancing side for each processing condition. Each colour in the EBSD maps represents a crystallographic orientation that is depicted in the hcp inverse pole figure (IPF) in the lower right corner of Figure 8. This is the IPF coloured map for the cast and β – FS processed material which is also representative of the IPF map for the mill-annealed and β – FS processed plate. The important information for the present study was actually the pole figures generated from the EBSD data. The α phase 0001 and $11\bar{2}0$ pole figures for all three samples in this study are shown in Figure 9. Only orientations with confidence indexes (CI) exceeding 0.1 were used in calculating the orientation distribution (OD), from which the pole figures were derived. In Figure 9, RD is parallel to the tool travel direction and TD points to the advancing side, whereas the direction normal to the plane of projection, ND, is parallel to the tool rotation axis. Most notable was the lack of any appreciable texture in the α/β – FS processed sample. The maximum intensity in this region of the sample was only about 2.7 times random. In some cases, several neighbouring equiaxed grains shared a similar orientation, but there was no textured region observed larger than approximately 3 μm or 4 μm. Some researchers have reported underlying simple shear, or alternatively, torsion textures in friction stir welded fcc [22, 23] and bcc materials [24, 25]. Simple shear textures are generally not strong because each grain is constantly rotating with respect to the sample reference frame. The appearance of texture is a result of certain orientations rotating more slowly with respect to the sample reference frame than others [26]. The location of the ideal orientations is dependent only on crystal symmetry. The ideal orientations have been determined for both bcc [27] and hcp materials [28] using polycrystal plasticity simulations. The lack of a distinct shear texture in the α/β – FS processed sample has been attributed to sampling an area of insufficient size. Only 1 100 grains contributed to the OD in the present study. Shear textures have been observed when larger areas were scanned and approximately 10 000 thousand grains were sampled, though the maximum intensities are still on the order of 2x random [29].

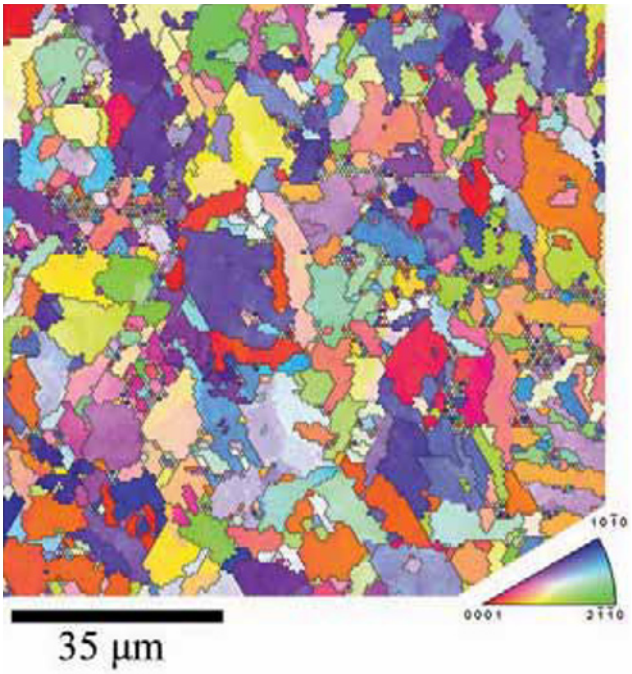

The tool travel direction is out of the plane of the page in this transverse section through the SZ on the advancing side.

Figure 8 – An inverse pole figure coloured map of the SZ in the cast and β – FSP plate

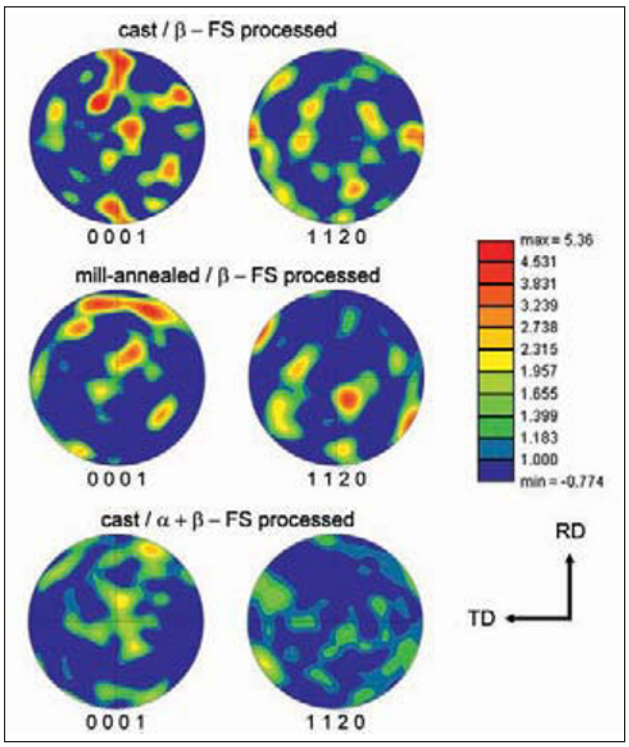

Equal area projections with intensities based on a maximum of 5.36 multiples of a random distribution in the mill-annealed and β – FS processed sample. RD is parallel to the tool travel direction and TD points to the advancing side.

Figure 9 – α phase pole figures generated from the EBSD data

The maximum intensity in the β – FS processed samples is generally higher, around 5 multiples of a random distribution. Since only the β phase is present during β – FSP, the α phase pole figures reflect the β → α + β transformation texture, which is governed by the Burgers orientation relationship (BOR). The BOR states that (0001)α ∥ {110}β and $<11\bar{2}0>$ ∥ <111>β. The β deformation texture should be reflected in the α transformation texture.

A full analysis is beyond the scope of the present article, but it is worth mentioning that after suitable rotations about ND and RD, it appears possible that the 0001 texture could be the result of <111> ∥ shear direction fibres in the β phase [27]. These rotations are -87.5° about ND, 7.5° about RD and -60° about ND and

12° about RD for the cast and mill annealed samples, respectively.

Attempts to determine β phase textures in the α/β – FS processed material were unsuccessful. Very fine scale secondary α was present in the β phase between the primary α grains. These acicular, secondary α platelets had size scales around 75 nm, which approached, or surpassed, the spatial resolution of the EBSD technique in Ti alloys. Further, electron backscatter diffraction patterns collected from the β phase are often diffuse and overlap with α phase patterns leading to improper indexing and low confidence indexes.

3.4 Fatigue behaviour

A preliminary investigation into the effect of FSP on the fatigue life of cast α/β– and β–FS processed was previously reported [7]. The samples were tested in the as – FS processed condition with no subsequent heat treatment. The results indicated that FS processed cast material possessed a fatigue life that was as much as an order of magnitude higher than that of as-cast material at constant stress amplitude. In the present work, several additional tests were conducted on the as-mill-annealed material as well as β – FS processed four point bend samples. The base material samples were oriented such that the longitudinal axis aligned with the transverse direction of the rolled plate. This orientation is the strongest orientation since the c-axis of the α phase typically lies in this direction in rolled plate material. The results, presented in Table 2, are consistent with those previously reported, which showed that FSP significantly increases the fatigue life. In Table 2, "MA" samples are the as-mill-annealed and MA-FS represent the samples that were friction stir processed.

An important parameter regarding the fatigue performance of α + β titanium alloys has been demonstrated to be the effective slip length of the material [1, 30]. The effective slip length is controlled by microstructural units such as colony size and α grain size. In the casting, the grain size is reduced from ~500 μm to about 1 μm after FSP. There is not a substantial reduction in slip length in the mill-annealed and β–FSP plate, yet a large increase in fatigue life is observed. The reasons for the increase in fatigue life are not entirely clear, but one source could be linked to the residual stresses. Karogal [13] and John *et al*. [31] have both reported compressive residual stresses in the surface and root of friction stir welded Ti-6Al-4V. These compressive residual stresses could be responsible for the observed increase in fatigue life by delaying crack initiation [1]. X-ray diffraction studies of the α/β – FS processed material [5] revealed both peak broadening and peak shift, which corresponded to non-uniform and uniform residual strain, respectively. While this was only a qualitative assessment, it suggested that residual stresses may be present in the α/β – FS processed condition.

At this point, it is not possible to make an assessment of the relative fatigue strength of mill annealed β –FS processed, cast β – FS processed, and cast α/β – FS processed due to the small number of samples available. Testing is underway on additional samples to generate complete S-N curves in order to validate these results. Samples that have been annealed to relieve any potential residual stresses are also being examined.

3.5 Tool wear effects

Tool contamination has been generally less of an issue in Al alloys than in titanium alloys. Most reports of successful FS welding and processing in higher temperature materials were in studies utilizing W-based alloy tools [5, 14, 24, 25]. The most tool wear has been reported to occur during plunging [32]. In the same study, the authors reported that at the constituent level there was no evidence of tool debris for the case where the SZ temperature exceeded the β transus during welding. However, there have also been observations of second phases containing the tool material in steel [33] and titanium [34] as well as discrete particles of the tool material [14, 34].

In the cast α/β – FS processed plate, it was previously reported the existence of an approximately 2.5 mm wide "stripe" of sub-micron sized W-rich particles surrounded by an increased volume fraction of β phase in the transverse direction through the SZ. The location of this "stripe" was approximately 0.70 mm below the surface and ran the entire length of the FS processed zone (Figure 10). It appeared that tool wear could be a concern during α/β – FSP. Some evidence of tool debris was noted in both the cast and mill annealed β – FS processed samples, but they were isolated and were not observed to cluster like the particles in Figure 10 b). It is important to point out that this is not sufficient evidence that the rate of tool wear during β – FSP was less than during α/β – FSP. The manifestation of tool wear may be different for α/β – and β – FS processed material. Tungsten is a β-eutectoid forming element with titanium. It is completely miscible in the solid body-centred cubic β phase but has an extremely low solid solubility in the hexagonal close packed α phase, only 0.2 wt% at 740 °C [35]. The complete miscibility of Ti and W, combined with higher processing temperatures, could allow the W particles to dissolve during β – FSP and become more homogeneously distributed throughout the SZ. The tool debris could be a limiting factor in post processing heat treatments since composition fluctuations can change phase transformation temperatures. In this case, local W enrichment would

Table 2 – Four-point bend fatigue testing results, R = 0.1, σ_{max} = 775 MPa, freq. = 20 Hz

Sample ID	MA-1	MA-2	MA-3	MA-4	MA-5	MA-FS1	MA-FS2
N_f	64 039	56 456	48 235	109 167	74 577	764 231	1 073 961

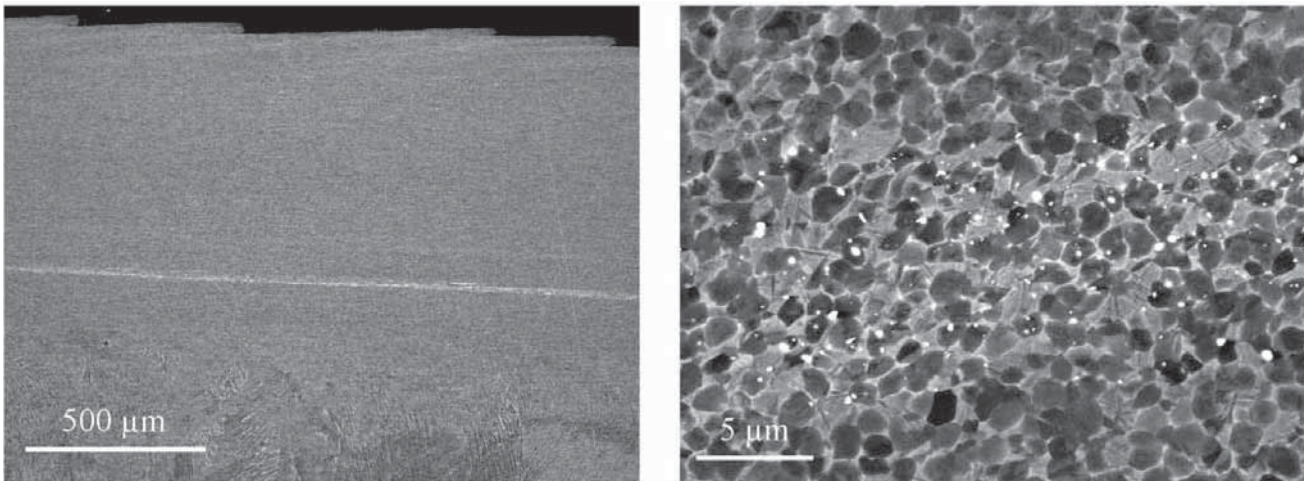

a) **b)**

The light coloured stripe in a) corresponds to an area of locally higher volume fraction of β phase as well as tungsten particles that are shown in higher magnification in b).

Figure 10 – A longitudinal section through the α/β – FSP material with the tool travel direction from right to left

suppress the β transus temperature and result in the formation of β flecks upon post processing heat treatment [34].

4 CONCLUSIONS

– Two different stir zone microstructures were produced from the same starting material by varying the processing parameters and thus changing total heat input. The resultant stir zone microstructure for α/β – FSP conditions was 1 µm equiaxed α; for β – FS processed conditions the stir zone microstructure was 15 µm colonies in 30 µm prior β grains.

– The equiaxed grains have the benefit of being finer than can be achieved in commercial manufacturing conditions, with substantially less microtexture, as evidenced by EBSD experiments.

– With respect to fatigue crack initiation resistance, the as-FS processed microstructure is promising, although residual stress effects have not been clearly disaggregated from microstructure effects. The reduction of the effective slip length from the large colony structure to the refined primary α grain size or the reduced colony size was at least partially responsible for the increase in fatigue life.

– Substantial tool wear was observed in the sub-β transus processed material. This could have consequences in high temperature applications or in the case of post processing heat treatment. By comparison, very little tool wear was observed when material was processed above the β transus.

REFERENCES

[1] Lutjering G., Williams J.C.: Titanium, Springer, New York, NY, 2003.

[2] Suresh S.: Fatigue of materials, 2nd ed., Cambridge University Press, New York, NY, 1998.

[3] Mishra R.S., Mahoney M.W., McFadden S.X., Mara N.A., Mukherjee A.K.: High Strain rate superplasticity in a Friction Stir Processed 7075 Al Alloy, Scripta Mat., 2000, vol. 42, pp. 163-168.

[4] Mishra R.S., Ma Z.Y.: Friction stir welding and processing, Mat. Sci. Eng. R, 2005, vol. 50, pp. 1-78.

[5] Pilchak A.L., Li Z.T., Fisher J.J., Reynolds A.P., Juhas M.C., Williams J.C.: The relationship between Friction Stir Processing (FSP) parameters and microstructure in investment cast Ti-6Al-4V, in Friction Stir Welding and Processing IV, R.S. Mishra, M.W. Mahoney, T.J. Lienert, and K.V. Jata, eds., TMS, Warrendale, PA, 2007, pp. 419-427.

[6] Pilchak A.L., Norfleet D.M., Juhas M.C., Williams J.C.: Friction Stir Processing of investment-cast Ti-6Al-4V: Microstructure and properties, in Materials Behavior Far From Equilibrium, Metall. Mater. Trans. A., 2008, 39A, pp. 1519-1524.

[7] Pilchak A.L., Juhas M.C., Williams J.C.: Microstructure and properties of investment cast Ti-6Al-4V: in The Proc. 11th International Conference on Titanium, Kyoto, Japan, 2007, Japan Institute of Metals, pp. 1723-1726.

[8] Oh-ishi K., Cuevas A.M., Swisher D.L., McNelley T.R.: The influence of friction stir processing on microstructure and properties of a cast nickel aluminum bronze material. THERMEC'2003, Mat. Sci. For., 2003, vols. 426-432, pp. 2885-90.

[9] Oh-Ishi K., McNelley T.R.: Microstructural modification of as-cast NiAl bronze by Friction Stir Processing. Metall. Mater. Trans. A., 2004, vol. 35A, pp. 2951-2961.

[10] Oh-ishi K., McNelley T.R.: The Influence of Friction Stir Processing parameters on microstructure of as-cast NiAl bronze, Metall. Mater. Trans. A., 2005, vol. 36A, pp. 1575-85.

[11] Oh-Ishi K., Zhilyaev A.P., McNelley T.R.: A microtexture investigation of recrystallization during Friction Stir Processing of as-cast NiAl bronze, Metall. Mater. Trans. A., 2006, 37A, pp. 2239-2251.

[12] Ramirez A.J., M.C. Juhas: Microstructural evolution in Ti-6Al-4V Friction Stir Welds, THERMEC'2003, Mat. Sci. For., 2003, vols. 426-432, pp. 2999-3004.

[13] Karogal N.: Microstructural evolution in Friction Stir Welding of Ti-6Al-4V, M.S. Thesis, The Ohio State University, Dept. Mat. Sci. Eng., 2002.

[14] Pilchak A.L., Juhas M.C., Williams J.C.: Microstructural changes due to Friction Stir Processing of investment cast Ti-6Al-4V, Metall. Mater. Trans. A., 2007, vol. 38, pp. 401-408.

[15] Bieler T.R., Semiatin S.L.: The origins of heterogeneous deformation during primary hot working of Ti-6Al-4V, Int. J. Plasticity, 2002, 18, pp. 1165-1189.

[16] Ma Z.Y., Pilchak A.L., Juhas M.C., Williams J.C.: Microstructural refinement and property enhancement of cast light alloys via friction stir processing, Scripta Materialia Viewpoint Set 43, 2008, vol. 58, iss. 5, pp. 361-366.

[17] Su J.-Q., Nelson T.W., Mishra R., Mahoney M.: Microstructural investigation of friction stir welded 7050-T651 aluminum, Acta Materialia, 2003, vol. 51, pp. 713-729.

[18] Humbert M., Wagner F., Moustafid H., Elsing C.: Determination of the orientation of a parent beta-grain from the orientations the inherited alpha-plates in the phase transformation from body-centered-cubic to hexagonal close-packed, J. Appl. Cryst., 1995, 28, pp. 571-576.

[19] N. Gey, M. Humbert, M.J. Philippe Y. Combres: Modeling the transformation texture of Ti-64 sheets after rolling in the beta-field. Mat. Sci. Eng. A., 1997, A230, pp. 68-74.

[20] Peters M., Gysler A., Lütjering G.: Influence of microstructure on the fatigue behavior of Ti-6Al-4V. Titanium '80 Science and Technology, Proceedings of the Fourth International Conference on Titanium, Kyoto, Japan, 1980, pp. 1777-1786.

[21] Yapici G.G., Karaman I., Luo Z.P.: Mechanical twinning and texture evolution in severly deformed Ti-6Al-4V at high temperatures, Acta Materialia, 2006, vol. 54, 14, pp. 3755-3771.

[22] Fonda R.W., Bingert J.F., Colligan K.J.: Texture and grain evolutions in a 2195 Friction Stir Weld, Proceedings of the Fifth International Symposium on Friction Stir Welding, Metz, France, September 14-16, 2004.

[23] Fonda R.W., Bingert J.F.: Microstructural evolution in the heat-affected zone of a Friction Stir Weld. Metall. Mater. Trans. A., 2004, vol. 35A, pp. 1487-1499.

[24] Reynolds A.P., Hood E., Tang W.: Texture in friction stir welds of Timetal 21S. Scripta Mat., 2005 vol. 52, pp. 491-4.

[25] Li Y., Hood E., Tang W., Reynolds A.P.: Friction stir welding of Timetal 21S, in K.V. Jata, M.W. Mahoney, R.S. Mishra, and T.J. Lienert (Eds.), Friction Stir Welding and Processing III, The Minerals, Metals and Materials Society, Warrendale, PA, 2005, pp. 81-9.

[26] Rollet A.D., Wright S.I.: in U.F. Kocks, C.N. Tome, and H.-R. Wenk (Eds.) Texture and Anisotropy: Preferred Orientation in Polycrystals and their Effect on Materials Properties, Cambridge University Press, Cambridge, UK, 1998, pp. 187.

[27] Baczynski J., Jonas J.J.: Texture development during the torsion testing of α-iron and two IF steels, Acta. mater.,1996, 44, 11, pp. 4273-4288.

[28] Beausir B., Toth L.S., Neale K.W.: Ideal orientations and persistence characteristics of hexagonal close pakked crystals in simple shear, Acta mater., 2007, 55, pp. 2695-2705.

[29] Pilchak A.L., The Ohio State University, unpublished research, 2007.

[30] Wegmann G., Albrecht J., Lütjering G., Folkers K.D., Liesner C.: Microstructure and mechanical properties of titanium castings, Z. Metallkd, 1997, 88, 10, pp. 764–773.

[31] John R., Jata K.V., Sadananda K.: Residual stress effects on near-threshold fatigue crack growth in friction stir welds in aerospace alloys, Int. J. Fatigue, 2003, 25, 9-11, pp. 939-948.

[32] Lienert T.J., Jata K.V., Wheeler R., Seetharaman V.: Friction Stir Welding of Ti-6Al-4V Alloys, in Proceedings of the Joining of Advanced and Specialty Materials III, ASM International, Materials Park, OH, USA, 2001, pp. 160-167.

[33] Klingensmith S., DuPont J.N., Marder A.R.: Microstructural characterization of a double-sided Friction Stir Weld on a superaustenitic stainless steel, Welding Journal, 2005, 84,5, pp. 77S-85S.

[34] Pilchak A.L., Juhas M.C., Williams J.C.: Observations of tool-workpiece interactions during Friction Stir Processing of Ti-6Al-4V, Metall. Mater. Trans. A., 2007, Vol. 38, No. 2, pp. 435-437.

[35] Landolt-Börnstein - Group IV Physical Chemistry, Volume 5: Pu-Re – Zn-Zr, Publisher: Springer-Verlag, Copyright 1998, pp.1-2.